The Lateral Ganglionic Eminence Does Not Generate Cortical Oligodendrocytes

Running title: The LGE does not generate cortical OLs

Jialin Li[1, #], Feihong Yang[2, #], Yu Tian[1, #], Ziwu Wang[1], Dashi Qi[3], Zhengang Yang[1], Jiangang Song[2], Jing Ding[1], Xin Wang[1, *] and Zhuangzhi Zhang[1, *]

[1]State Key Laboratory of Medical Neurobiology and MOE Frontiers Center for Brain Science, Institutes of Brain Science, and Department of Neurology, Zhongshan Hospital, Fudan University, Shanghai 200032, P.R. China.

[2]Department of Anesthesiology, Shuguang Hospital Affiliated with Shanghai University of Traditional Chinese Medicine, Shanghai 201203, P.R. China

[3]Center for Clinical Research and Translational Medicine, Yangpu Hospital, School of Medicine, Tongji University, Shanghai 200090, P.R. China.

[#]These authors contributed equally to this work.

***Correspondence**

Xin Wang,

Email: wang.xin@zs-hospital.sh.cn

Zhuangzhi Zhang,

Email: zz_zhang@fudan.edu.cn

Abstract

The emergence of myelinating oligodendrocytes represents a pivotal developmental milestone in vertebrates, given their capacity to ensheath axons and facilitate the swift conduction of action potentials. It is widely accepted that cortical oligodendrocyte progenitor cells (OPCs) arise from medial ganglionic eminence (MGE), lateral/caudal ganglionic eminence (LGE/CGE) and cortical radial glial cells (RGCs). Here, we used two different fate mapping strategies to challenge the established notion that the LGE generates cortical OPCs. Furthermore, we used a *Cre-loxP*-dependent exclusion strategy to reveal that the LGE/CGE does not give rise to cortical OPCs. Additionally, we showed that specifically eliminating MGE-derived OPCs leads to a significant reduction of cortical OPCs. Together, our findings indicate that the LGE does not generate cortical OPCs, contrary to previous beliefs. These findings provide a new view of the developmental origins of cortical OPCs and a valuable foundation for future research on both normal development and oligodendrocyte-related disease.

Keywords: Oligodendrocyte, LGE, MGE, Migration, Cortex, Fate mapping

Introduction

Oligodendrocytes (OLs) are one of the most abundant cell types in the mammalian neocortex. The emergence of myelination OLs in vertebrates is a major event in the evolution of the central nervous system (CNS), as these cells play a crucial role in enhancing axonal insulation and the conduction of neural impulses. Previously, they have been described as support cells that myelinate axons and play essential roles in the function of neocortical circuits. Myelin loss or dysfunction is associated with many disorders, such as multiple sclerosis, depression and pediatric leukodystrophies[1,2].

During CNS development, OLs originate from oligodendrocyte precursor cells (OPCs), which arise from different regions of the embryonic neural tube. OPCs proliferate and migrate away from the ventricular germinal zones (VZ) into developing gray and white matter before differentiating into mature OLs[3,4]. The developmental origin of cortical oligodendrocytes has been extensively studied in the CNS, especially in the neocortex[5-8]. A landmark study[9] demonstrated that cortical OPCs are generated in three waves, starting with a ventral wave, gradually transitioning to more dorsal origins. The first wave of cortical OPCs is derived from the medial ganglionic eminence (MGE) or the anterior entopeduncular area (AEP) at embryonic day E12.5 (*Nkx2.1*$^{+}$ lineage). The second wave of cortical OLs is derived from the lateral/caudal ganglionic eminences (LGE/CGE) at E15.5 (*Gsx2*$^{+}$/*Nkx2.1*$^{-}$ lineage). The final wave occurs at P0, when OPCs originate from cortical glial progenitor cells (*Emx1*$^{+}$

lineage). Our recent studies[10,11], however, challenge the notion that cortical OLs are generated in these three waves[9,12-14], as the cortical glial progenitor cells were also found to express *Gsx2*, which was known to be exclusively expressed in the developing subpallium[15-17], after E16.5[11]. Therefore, *Gsx2*$^{+}$*/Nkx2.1*$^{-}$ lineage OLs may not represent LGE-derived cortical OLs. To date, whether the LGE generates cortical OPCs (OLs) during cortical development remains an unanswered question in the field of developmental neuroscience.

The present study was undertaken to answer this question. We carried out distinct fate mapping experiments and intersectional lineage analyses to reveal that cortical OPCs do not derive from the LGE. First, using in utero electroporation (IUE) to target the LGE in a *Cre* recombinase-dependent *IS* (*Rosa-CAG-LSLFrt-tdTomato-Frt-EGFP*) reporter mouse line[18], we found that LGE-derived OPCs produced striatal OLs rather than cortical OLs. Second, by combining the PiggyBac transposon system with IUE, we found that no traced cells migrated into the cortex from the LGE. Third, by crossing the *Nkx2.1-Cre* and *Emx1-Cre* mouse lines with an *H2B-GFP* reporter mouse line, we found that nearly all cortical OPCs originated from *Nkx2.1-Cre* or *Emx1-Cre* lineage cells. Finally, we analyzed *Olig2*-conditional knockout mice (*Nkx2.1-Cre; Olig2*$^{F/F}$ mice*)*, and found that the number of cortical OPCs was significantly reduced from E14.5 to E16.5. These results indicated that the MGE was the sole ventral source of cortical OPCs. Taken together, our findings suggest that

the LGE does not give rise to cortical OPCs (OLs) during neocortical development.

In summary, our findings collectively indicate that the MGE is the primary ventral source of cortical OPCs (OLs) and that the LGE does not generate cortical OPCs, challenging the conventional view that the LGE generates cortical OPC (OL) populations during cortical development. This research advances our understanding of CNS development and presents a new perspective on the origins of cortical OPCs (OLs).

Results

Fate mapping of LGE-derived OPCs by combining IUE with a *Cre* recombinase-dependent *IS* reporter

OPCs initially emerge in the ventral VZ of the MGE and can be labeled by platelet-derived growth factor receptor (a-subunit, *Pdgfra*) around E12.5. We hypothesized that if the LGE generated cortical OPCs, the *Pdgfra*$^+$ cell migration stream from the LGE to the cortex could be observed during cortical development. To confirm this speculation, we conducted a detailed analysis of *Pdgfra* mRNA expression using *in situ* hybridization (ISH). Our results showed that there was no observable *Pdgfra*$^+$ cell migration stream from the LGE to the cortex from E13.5 to P0 (Figure 1A). Next, we used *Cre* recombinases in combination with an *IS* reporter mouse line[18] to fate map LGE-derived OPCs (OLs). We delivered *pCAG-Cre* plasmids specifically into the LGE VZ of *IS*

reporter mouse embryos at E13.5 by IUE (Figures 1B-C). In this experiment, cells generated from electroporated neural stem cells (NSCs) expressed tdTomato (tdT). Interestingly, we observed many tdT$^+$ cells throughout the whole LGE (striatum) at E18.5. In contrast, there were very few tdT$^+$ cells detected in the cortex (Figure 1D). OPCs express *Olig2*, *Sox10*, *Pdgfra* and NG2 (*Cspg4*) and mature neurons express NeuN [19-25]. To determine the identity of the tdT$^+$ cells, we performed double staining of tdT with OLIG2, SOX10, PDGFRA, NG2 (CSPG4) and NeuN. Within the cortex, tdT$^+$ cells did not express OPC marker genes but express NeuN; however, tdT$^+$ cells expressed OPC marker genes and NeuN in the striatum (Figure 1E). We also delivered *pCAG-Cre* plasmids specifically into the LGE VZ of *IS* reporter mice at P0 by IUE and analyzed these mice at P49 (Figure 1F) to investigate whether the LGE generates cortical OLs at a later developmental stage. Our results showed that LGE progenitors generate LGE OLs and astrocytes, which expressed *Sox10* and *Sox9*, respectively (Figure 1F).

To further determine whether LGE-derived OPCs migrate into the cortex after E18.5, we used the same strategy as mentioned above (Figure S1A). We observed that at P10, the majority of the tdT$^+$ cells were located in the striatum, whereas very few tdT$^+$ cells were located in the neocortex (Figure S1B). All tdT$^+$ cells in the neocortex expressed NeuN but did not express OLIG2 (Figure S1C). In fact, tdT$^+$ cells in the neocortex did not express OPC marker genes; instead, they expressed NeuN in the neocortex. In contrast, tdT$^+$ cells in the

striatum expressed OPC marker genes (*Olig2*, *Sox10* and *Pdgfra*) and NeuN (Figure S1D), consistent with our observation at E18.5 (Figure 1E). We also found that tdT$^+$ cells expressed the astrocyte marker ALDH1L1 in the striatum at P10 (Figure S1D). Furthermore, through consecutive tissue sectioning and 3D reconstruction, we revealed that the traced cells tended to be localized in the striatum (Figure S1F). Collectively, our findings indicated that the LGE gives rise to striatal OLs, neurons and astrocytes, but not cortical OLs.

Lineage tracing of LGE-derived OPCs by combining IUE with the PiggyBac transposon system

To further investigate whether the LGE generates cortical OPCs during cortical development, we employed an alternative fate mapping strategy by combining IUE with the PiggyBac transposon system to map the fate of OPCs derived from LGE. This approach utilized a transposase enzyme (helper plasmid) to integrate the *H2B-GFP* sequence from a donor plasmid into the genome of the in utero electroporated LGE progenitors along the lateral ventricular zone. The *H2B-GFP* reporter vector was delivered specifically into the LGE VZ of wild-type embryos at E13.5 by IUE, and these embryos were examined at E18.5 or P10 (Figures 2A-B). In this system, most traced cells (GFP$^+$) were located in the striatum, and very few traced cells were observed in the cortex (Figures 2C and E). Usually, a small population of RGCs located in the dorsal LGE or lateral/ventral pallium was labeled by IUE. These RGCs

mainly migrated to the lateral/ventral pallium and amygdala (Figure 2C). We did not observe any GFP^+ cells that were OPCs in the dorsal cortex, as these cells did not express OLIG2, SOX10 or PDGFRA (Figure 2D). Instead, they expressed NeuN (Figure 2D). In contrast, GFP^+ cells expressed OLIG2, SOX10, PDGFRA and NeuN in the striatum at E18.5 (Figure 2D). The same results were also observed at P10 (Figure 2E). Again, our findings strongly suggested that the LGE does not generate cortical OPCs.

An exclusion strategy revealed that cortical OPCs do not originate from the LGE/CGE

While distinct fate mapping strategies provided evidence that the LGE did not generate cortical OPCs during cortical development, there remained a possibility that a small population of LGE RGCs or progenitors might generate a subpopulation of cortical OPCs at specific time points. To address this possibility, we crossed the *Emx1-Cre*[26-28], *Nkx2.1-Cre*[29] and *H2B-GFP*[18] mouse lines to generate *Emx1-Cre; Nkx2.1-Cre; H2B-GFP* mice. Because *Emx1-Cre* was specifically expressed in cortical RGCs[26] and *Nkx2.1-Cre* was specifically expressed in MGE/AEP RGCs[29], cortical OPCs were traced (GFP^+ cells) in using *Emx1-Cre; Nkx2.1-Cre; H2B-GFP* mice. GFP^- cell OPCs, on the other hand, were considered as LGE/CGE-derived cortical OPCs (OLs) (Figures 3A-B).

A previous report[9] suggested that cortical OPCs originate from MGE, LGE/CGE and cortical RGCs. When MGE-derived cortical OPCs were eliminated, LGE/CGE-derived cells accounted for approximately 50% of cortical OPCs at P10. To confirm these findings, we performed double staining of GFP with OPC marker genes, such as *Sox10* and *Pdgfra* in *Emx1-Cre; Nkx2.1-Cre; H2B-GFP* mice (Figure 3C). We observed that the majority of OPCs or OLs were colabeled with GFP in *Emx1-Cre; Nkx2.1-Cre; H2B-GFP* mice at P10 (Figure 3C). Statistical analysis showed that only approximately 2% of OPCs were GFP^- cells, and they were possibly derived from the LGE/CGE (Figures 3D-E), which was consistent with our observation at P0 (Figures 3G-I). Importantly, the expression of *Nkx2.1-Cre* is lower within the dorsalmost region of the MGE than in other *Nkx2.1*-expressing regions[29]. Thus, these GFP^- OPCs (~2%) may be derived from the dorsal MGE rather than from the LGE/CGE. Using this approach, we revealed that nearly all cortical OLs/OPCs were derived from MGE/AEP and cortical RGCs. Taken together, our findings indicated that the LGE/CGE did not generate cortical OLs, or that if they do, the number is negligible.

The MGE/AEP was the sole ventral source of the cortical OPCs

Olig2, a basic helix-loop-helix transcription factor, plays a critical role in the regulation of OPC fate determination. To investigate the role of *Olig2* in the MGE, we crossed *Nkx2.1-Cre* mice with *Olig2* $^{F/+}$ mice to eliminate *Olig2*

expression in the SVZ/VZ of the MGE/AEP (Figures 4A-B). We referred to the conditional mutants as *Olig2-NCKO* mice. A previous study[9] showed that MGE/AEP-derived OPCs migrate into the cortex around E14.5, and LGE/CGE-derived OPCs migrate into cortex around E15.5. We assumed that the MGE/AEP was the sole ventral source of cortical OPCs, and that inhibiting MGE/AEP-derived OPC generation would therefore significantly reduce the number of cortical OPCs at E16.5. To test this possibility, we analyzed *Olig2-NCKO* mice, in which the generation of MGE/AEP-derived OPCs was inhibited. Our results showed that the expression of OPC marker genes, such as *Sox10* and *Pdgfra* was significantly reduced (> 10-fold) in the cortex of *Olig2-NCKO* mice, compared to the control mice at E14.5 and E16.5 (Figures 4C-E). Considering the recombination efficiency of the CRE enzyme, the limited presence of residual OPCs in the cortex of *Olig2-NCKO* mice may be arise from the MGE/AEP. Indeed, we observed few PDGFRA-positive cells in the MGE/AEP of the *Olig2-NCKO* mice (Figure 4F). Altogether, our findings indicated that the MGE/AEP was the sole ventral source of cortical OPCs.

Discussion

It is widely accepted in the field of developmental neuroscience that cortical oligodendrocyte precursor cells (OPCs) originate from three regions: the MGE/AEP, LGE/CGE and cortex. However, in the current study, we re-examined the developmental origins of cortical OPCs using diverse

strategies. Our findings show that cortical OPCs do not come from the LGE/CGE, contrary to previous reports[9,12], which suggested that the LGE/CGE generates cortical OPCs (Figure 4G). In fact, no cortical OPCs migrating from the LGE to the cortex were observed via our two fate mapping strategies. Furthermore, an exclusion strategy suggested that the LGE/CGE were not responsible for generating cortical OPCs. In addition, according to our study of *Olig2-NCKO* mice, MGE/AEP seems to be the sole ventral source of cortical OPCs during neocortical development. Overall, these findings provide evidence that the LGE does not generate cortical OPCs in the mouse brain.

Why the LGE cannot generate cortical OPCs during cortical development

OLs are specialized cells of the CNS that produce myelin, a multilayered membrane that spirally enwraps axons and facilitates rapid nerve conduction. Recent studies have shown that cortical OLs are heterogeneous, as there are transcriptionally distinct subpopulations of cortical OLs during development and disease[8,30-32]. Indeed, OLs are derived from distinct OPC pools, which acquire different abilities to respond to demyelination[9,33]. In the spinal cord, the developmental origin of OLs has been hotly debated for many years. Some groups believed that OLs originate only from the ventral neural tube, whereas others tend to support multiple origins[12,34-36]. Currently, it is generally accepted that spinal cord OLs are derived from two origins: the ventral region and dorsal

region. One pioneering study[9] purported that, in the forebrain, cortical OLs derive from multiple origins, such as the MGE, LGE and cortex.

In general, the specification of OLs depends on SHH protein released from the notochord and floor plate, as *Shh* expression is both necessary and sufficient for OL generation in the spinal cord[37]. As in the spinal cord, OL generation in the cortex is also dependent on the *Shh* signaling pathway[38]. During MGE development, *Nkx2.1* and *Six3* promote SHH secretion. Furthermore, the early-born neurons of the MGE also secrete SHH protein before E14.5[39]. Thus, the high levels of SHH in the MGE contribute to the generation of OPCs from RGCs. In contrast, *Shh* signaling pathway activity is very weak in the LGE at the early stage (before E14.5). As the level of SHH gradually increases in the LGE, this results in a shift from neurogenesis to gliogenesis after E15.5, and the large number of the striatal neurons may block the migration of OPCs into the neocortex[40,41]. In summary, the process of cortical OL generation can be summarized as follows: First, the time window during which the MGE generates OLs is very brief, perhaps occurring before MGE neurogenesis. The high level of SHH in the MGE allows for the production of a small population of cortical OPCs around E12.5. Subsequently, multipotent intermediate progenitors begin to express DLX transcription factors resulting in ending the generation of OPCs in the MGE[42-44]. Second, radial glial cells (RGCs) undergo a gradual transition from neurogenesis to gliogenesis around E15.5, driven by the progressive elevation of SHH levels in the LGE.

However, the LGE had already generated a substantial number of neurons during this period, blocking the migration of OPCs into the cortex. Finally, with the gradual increase of SHH concentration, cortical RGCs begin to cease neurogenesis and shift toward gliogenesis after E16.5[10,40,45]. Therefore, the generation of cortical OPCs (OLs) is regulated by both precise temporal and spatial patterning, which is strictly dependent on the local environment.

Cortical-derived OLs/OPCs make up the majority of the cortical OLs/OPCs in the adult brain

During the early development of the cortex, both pallium and subpallium can generate cortical OPCs[9,46]. Interestingly, most of the ventral-derived OPCs, particularly MGE-derived OPCs/OLs, are eventually eliminated due to the continued expansion of dorsal-derived OPCs in the adult cortex[6,9]. It appears that OPCs generated later in development may possess a competitive advantage over their earlier-generated counterparts. Indeed, human glial progenitor cells (hGPCs) engrafted neonatally or transplanted into the adult mouse brain can effectively disperse throughout the forebrain, differentiate into mature OLs and remyelinate the demyelinated adult brain[1,47]. These findings indicate that OPCs generated later in development have the ability to take over for earlier-generated OPCs in the adult brain.

Based on the present work and other studies[8,9,46], cortical-derived OPCs probably constitute the majority of cortical OPCs, including mature cortical OLs.

Thus, OLs may function as a homogeneous population in the adult forebrain. In fact, the number of LGE/CGE-derived cortical OPCs may also gradually decrease in the adult brain, as reported by Lui et al[6]. However, Lui et al. did not analyze LGE-derived and MGE-derived OPCs separately. Therefore, they did not exclude the possibility that the LGE/CGE does not generate cortical OPCs. In summary, cortical OPCs/OLs comprise MGE-derived and cortical RGC-derived OPCs/OLs during the neonatal stage. However, only cortical-derived OPCs/OLs remain in the adult cortex.

Our study provides strong evidence that the LGE does not give rise to cortical OPCs/OLs during forebrain development. Thus, our findings provide new evidence about the developmental origins of cortical OLs, which may guide future research on both normal development and disease.

Methods

Animals

All experiments conducted in this study were in accordance with the guidelines of Fudan University. We used *Emx1-Cre*[26,27], and *Nkx2.1-Cre*[29] mice, in conjunction with either *Rosa-H2B-GFP*[18] or *Rosa-IS*[18] for genetic fate mapping. *Olig2*$^{F/+}$ mice were generated via the CRISPR/Cas9 strategy. LoxP sites flanked the coding region of exons 1 and 2. Wild-type mice or littermates without the *Cre* allele were used as controls. All mice were maintained on a mixed genetic background (C57BL/6J and CD1). The mice were allowed access to water and food ad libitum and maintained on a 12-hour light/dark cycle. The day of vaginal plug detection was considered embryonic day 0.5 (E0.5), and the day of birth was defined as postnatal day 0 (P0). Both male and female mice were used in all experiments.

Tissue preparation

Postnatal mice were deeply anesthetized and perfused intracardially thoroughly with ice-cold PBS followed by 4% paraformaldehyde (PFA). Embryos were harvested from deeply anesthetized pregnant mice. All brains were fixed overnight in 4% PFA at 4°C, cryoprotected in 30% sucrose for at least 24 hours, embedded in optimal cutting temperature (O.C.T.) (Sakura Finetek) on dry ice and ethanol slush and preserved at -80℃. All frozen

mouse tissues were sectioned into 20 μm thick sections unless specifically mentioned and stained on glass slides.

Plasmid Construction

The *pCAG-Cre* vector was constructed as reported elsewhere. The coding sequence of *Cre* in the *pCAG-Cre* vector was replaced by the *PiggyBac transposase* to construct the *pCAG-PiggyBac transposase* vector. The coding DNA sequence (CDS) of *Cre* in the *pCAG-Cre* vector was replaced by *H2B-GFP* from the *Rosa-H2B-GFP* mouse strain to construct the *PB-pCAG-H2B-GFP* vector. The inverted terminal repeat (ITR) sequence of the PiggyBac transposon was cloned upstream of the *CAG* promoter and downstream of the beta-globin polyA sequence for recognition by the PiggyBac transposase.

In utero electroporation (IUE)

In utero electroporation (IUE) of wild-type or IS embryos was performed at E13.5. The *pCAG-Cre* (Addgene #13775), *pCAG-GFP* (Addgene #11150), *pCAG*-PiggyBac transposase or *PB- pCAG-H2B-GFP* (final concentration: 1-2 μg/μL) plasmid was mixed with 0.05% Fast Green (Sigma) and injected into the lateral ventricle of embryos (0.5 μL per embryo) using a beveled glass micropipette. Five electrical pulses (duration: 50 ms) were applied at 42 V across the uterine wall with a 950 ms interval between pulses. Electroporation

was performed using a pair of 5 mm platinum electrodes (BTX, Tweezertrode 45-0488, Harvard Apparatus) connected to an electroporator (BTX, ECM830). The embryos were analyzed at E18.5 and P10.

Immunofluorescence

The sections were first washed with 0.05 M TBS for 10 min, incubated in Triton-X-100 (0.5% in 0.05 M TBS) for 30 min at room temperature (RT), and then incubated with blocking solution (5% donkey serum +0.5% Triton-X-100 in 0.05 M TBS, pH= 7.2) for 2 h at RT. The primary antibodies were diluted in 5% donkey serum, incubated overnight at 4°C, and then rinsed 3 times with 0.05 M TBS.

Secondary antibodies (1:500, all from Jackson ImmunoResearch) matching the appropriate species were added and incubated for 2-4 h at RT. Fluorescently stained sections were then washed 3 times with 0.05 M TBS for 10 min. The sections were then stained with 4',6-diamidino-2-phenylindole (DAPI) (1:3000, Sigma) diluted in TBS for 1 min and then finally rinsed three more times with TBS. The sections were then coverslipped with Gel/Mount (Biomeda, Foster City, CA). The primary antibodies used in this study are shown in the key resource table.

***In situ* hybridization (ISH)**

ISH was performed on 20-μm cryosections using digoxigenin riboprobes as previously described [48]. The sections were first postfixed in 4% PFA for 20 min. mRNA *in situ* hybridization was performed as previously described[49]. The probes were constructed from cDNA isolated from the wild-type mouse brain and amplified by PCR using the following primers:

Probe Name	Primer Sequence
Pdgfra	Primer F: TGGCCAGCAATGTCTCAAAT
	Primer R: TCCTTTCAAGCATGGGGACA

3D Reconstruction

Images of serial coronal sections along the rostral–caudal axis were collected via an Olympus VS 120 microscope using a 10X objective and used by Amira as a formwork for reconstruction. The coordinates of each labeled cell (tdT+) in the brain were determined. A stereotaxic mouse brain atlas was used to locate the brain anatomical structures where the labeled cells were positioned.

Image acquisition and statistical analysis

Images for quantitative analyses were acquired with an Olympus VS 120 microscope using a 10X objective. Bright-field images were acquired with an Olympus VS 120 microscope using a 10X objective. Other fluorescence images were taken with the Olympus FV3000 confocal microscope system

using 20× or 40× objectives. The images were merged, cropped and optimized in Adobe Photoshop and Adobe Illustrator without distorting the original visual information.

Analyses were performed using Microsoft Excel. Unpaired t test was used to determine statistical significance. All quantitative data are presented as the mean ± SEM. Differences with *p* values < 0.05 were considered significant. For quantification of $SOX10^+$, $PDGFRA^+$ and GFP^+ cells in the cortex at E18.5 and P10, six anatomically matched 20-μm thick coronal sections were selected (n = 6 mice per group). We counted $SOX10^+$, $PDGFRA^+$ and GFP^+ cells in the cortex under a 20X objective lens. The data are presented as the number of $SOX10^+$, $PDGFRA^+$ and GFP^+ cells per section for each cortex.

For quantification of $SOX10^+$ and $PDGFRA^+$ cells in the dorsal cortex at E14.5 and E16.5, five or six anatomically matched 20-μm thick coronal sections were selected (n = 6, E14.5; n=5, E16.5). We counted $SOX10^+$ and $PDGFRA^+$ cells in the cortex under a 20X objective lens. The data are presented as the number of $SOX10^+$ and $PDGFRA^+$ cells per section for each cortex.

Key resource table

Reagent or Resource	Source	Identifier
Antibodies		
Chicken Anti-GFP	Aves Labs	GFP-1020, 1:3000

Rabbit Anti-ALDH1L1	Abcam	ab87117, 1:1000
Rabbit Anti- OLIG2	Oasis Biofarm	OB-PRB009, 1:500
Rat Anti-OLIG2	Oasis Biofarm	OB-PRT020, 1:500
Mouse Anti-OLIG2	Millipore	MABN50, 1:1000
Rabbit Anti- OLIG2	Millipore	AB9610, 1:1000
Goat Anti-SOX10	R&D Systems	ab442208, 1:500
Guinea Pig Anti-SOX10	Oasis Biofarm	OB-PGP001, 1:1000
Rabbit Anti-PDGFRA	Oasis Biofarm	OB-PRB051, 1:800
Rabbit Anti-NeuN	Bioscience	R-3770-100, 1:1000
Rabbit Anti-NeuN	Oasis Biofarm	OB-PRB039, 1:1000
Guinea Pig Anti-NG2	Oasis Biofarm	OB-PGP002, 1:1000

Experimental models

Mouse: C57BL/6	Department of Laboratory Animal Science at Fudan University	http://10.107.12.196/

Mouse: CD1	Department of Laboratory Animal Science at Fudan University	http://10.107.12.196/
Mouse: IS reporter	The Jackson Laboratory	Stock No. 028582
Mouse: Olig2$^{F/+}$	This manuscript	N/A; available from the authors
Mouse: *Nkx2.1-Cre*	The Jackson Laboratory	Stock No. 008661
Mouse: *Emx1-Cre*	The Jackson Laboratory	Stock No. 005628

Recombinant DNA

pCAGIG	Addgene	Cat#11159
pGL4.10	Promega	Cat#E6651
pGL4.23	Promega	Cat#E8411

All secondary antibodies were from Jackson ImmunoResearch Labs.

Secondary Antibodies	Cat Number	Dilution
Alexa®488-Conjugated Affinipure Donkey Anti-Chicken IgY^{++} (IgG) (H^{+}L)	703-545-155	1:500
Cy^{TM}3-Conjugated Affinipure Donkey Anti-Rabbit IgG (H^{+}L)	711-165-152	1:500
Alexa®647-Conjugated Affinipure Donkey Anti-Rat IgG (H+L)	712-605-153	1:500

Alexa®647-Conjugated Affinipure Donkey Anti-Goat IgG (H^+L)	705-605-147	1:500
Alexa®488-Conjugated Affinipure Donkey Anti-Rabbit IgG (H^+L)	711-545-152	1:500
Cy™3-AffiniPure Donkey Anti-Goat IgG (H^+L)	705-505-147	1:500
Cy™3-AffiniPure Donkey Anti-Rat IgG (H^+L)	712-165-150	1:500
Cy™3-AffiniPure Donkey Anti-Guinea Pig IgG (H^+L)	706-165-148	1:500

Acknowledgements

This work was supported by the Ministry of Science and Technology of China (STI2030-2021ZD0202300), National Natural Science Foundation of China (NSFC 31820103006, 82271197, 81974175 and 32200776), Shanghai Municipal Science and Technology Major Project (No. 2018SHZDZX01), ZJ Lab, and Shanghai Center for Brain Science and Brain-Inspired Technology.

Data availability statement

The data that support the findings of this study are available from the corresponding author upon reasonable request.

Potential conflicts of interest

We declare that there is no conflict of interest.

Author contributions

J.L., F.Y. and Y.T. performed all experiments and analyzed data. Z.W., and D.Q. helped to conduct experiments and analyze the data. Z.Y. and Z.Z. designed the experiments and analyzed the results. Z.Z. wrote this manuscript. Z.Y., J.S., J.D., X.W. and Z.Y. help to review this manuscript.

References

1 Goldman, S. A., Mariani, J. N. & Madsen, P. M. Glial progenitor cell-based repair of the dysmyelinated brain: Progression to the clinic. *Semin Cell Dev Biol* **116**, 62-70, doi:10.1016/j.semcdb.2020.12.004 (2021).

2 Zhou, B., Zhu, Z., Ransom, B. R. & Tong, X. Oligodendrocyte lineage cells and depression. *Mol Psychiatry* **26**, 103-117, doi:10.1038/s41380-020-00930-0 (2021).

3 Miller, R. H. Oligodendrocyte origins. *Trends Neurosci* **19**, 92-96, doi:10.1016/s0166-2236(96)80036-1 (1996).

4 Huang, W. *et al.* Origins and Proliferative States of Human Oligodendrocyte Precursor Cells. *Cell*, doi:10.1016/j.cell.2020.06.027 (2020).

5 Allen, D. E. *et al.* Fate mapping of neural stem cell niches reveals distinct origins of human cortical astrocytes. *Science* **376**, 1441-1446, doi:10.1126/science.abm5224 (2022).

6 Liu, R. *et al.* In Vivo Clonal Analysis Reveals Development Heterogeneity of Oligodendrocyte Precursor Cells Derived from Distinct Germinal Zones. *Advanced Science* **8**, doi:10.1002/advs.202102274 (2021).

7 Shen, Z. *et al.* Distinct progenitor behavior underlying neocortical gliogenesis related to tumorigenesis. *Cell Rep* **34**, 108853, doi:10.1016/j.celrep.2021.108853 (2021).

8 Marques, S. *et al.* Transcriptional Convergence of Oligodendrocyte Lineage Progenitors during Development. *Dev Cell* **46**, 504-517 e507, doi:10.1016/j.devcel.2018.07.005 (2018).

9 Kessaris, N. *et al.* Competing waves of oligodendrocytes in the forebrain and postnatal elimination of an embryonic lineage. *Nat Neurosci* **9**, 173-179, doi:10.1038/nn1620 (2006).

10 Li, X. *et al.* Decoding Cortical Glial Cell Development. *Neurosci Bull* **37**, 440-460, doi:10.1007/s12264-021-00640-9 (2021).

11 Zhang, Y. *et al.* Cortical Neural Stem Cell Lineage Progression Is Regulated by Extrinsic Signaling Molecule Sonic Hedgehog. *Cell Reports* **30**, 4490-4504.e4494, doi:10.1016/j.celrep.2020.03.027 (2020).

12 Richardson, W. D., Kessaris, N. & Pringle, N. Oligodendrocyte wars. *Nat Rev Neurosci* **7**, 11-18, doi:10.1038/nrn1826 (2006).

13 Rowitch, D. H. & Kriegstein, A. R. Developmental genetics of vertebrate glial-cell specification. *Nature* **468**, 214-222, doi:10.1038/nature09611 (2010).

14 Bergles, D. E. & Richardson, W. D. Oligodendrocyte Development and Plasticity. *Cold Spring Harb Perspect Biol* **8**, a020453, doi:10.1101/cshperspect.a020453 (2015).

15 Chapman, H. *et al.* Gsx transcription factors control neuronal versus glial specification in ventricular zone progenitors of the mouse lateral ganglionic eminence. *Dev Biol* **442**, 115-126, doi:10.1016/j.ydbio.2018.07.005 (2018).

16 Chapman, H., Waclaw, R. R., Pei, Z., Nakafuku, M. & Campbell, K. The homeobox gene Gsx2 controls the timing of oligodendroglial fate specification in mouse lateral ganglionic eminence progenitors. *Development* **140**, 2289-2298, doi:10.1242/dev.091090 (2013).

17 Wen, Y. *et al.* Transcription Factor VAX1 Regulates the Regional Specification of the Subpallium Through Repressing Gsx2. *Molecular Neurobiology* **58**, 3729-3744, doi:10.1007/s12035-021-02378-x (2021).

18 He, M. *et al.* Strategies and Tools for Combinatorial Targeting of GABAergic Neurons in Mouse Cerebral Cortex. *Neuron* **91**, 1228-1243, doi:10.1016/j.neuron.2016.08.021 (2016).

19 Sun, T. *et al.* Olig bHLH proteins interact with homeodomain proteins to regulate cell fate acquisition in progenitors of the ventral neural tube. *Current biology : CB* **11**, 1413-1420, doi:10.1016/s0960-9822(01)00441-9 (2001).

20 Zhou, Q., Choi, G. & Anderson, D. J. The bHLH transcription factor Olig2 promotes oligodendrocyte differentiation in collaboration with Nkx2.2. *Neuron* **31**, 791-807, doi:10.1016/s0896-6273(01)00414-7 (2001).

21 Lu, Q. R. *et al.* Common developmental requirement for Olig function indicates a motor neuron/oligodendrocyte connection. *Cell* **109**, 75-86, doi:10.1016/s0092-8674(02)00678-5 (2002).

22 Finzsch, M., Stolt, C. C., Lommes, P. & Wegner, M. Sox9 and Sox10 influence survival and migration of oligodendrocyte precursors in the spinal cord by regulating PDGF receptor alpha expression. *Development* **135**, 637-646, doi:10.1242/dev.010454 (2008).

23 Reiprich, S. *et al.* Transcription factor Sox10 regulates oligodendroglial Sox9 levels via microRNAs. *Glia* **65**, 1089-1102, doi:10.1002/glia.23146 (2017).

24 Kucharova, K. & Stallcup, W. B. The NG2 proteoglycan promotes oligodendrocyte progenitor proliferation and developmental myelination. *Neuroscience* **166**, 185-194, doi:10.1016/j.neuroscience.2009.12.014 (2010).

25 Sanchez-Gonzalez, R., Bribian, A. & Lopez-Mascaraque, L. Cell Fate Potential of NG2 Progenitors. *Sci Rep* **10**, 9876, doi:10.1038/s41598-020-66753-9 (2020).

26 Gorski, J. A. *et al.* Cortical excitatory neurons and glia, but not GABAergic neurons, are produced in the Emx1-expressing lineage. *J Neurosci* **22**, 6309-6314, doi:10.1523/JNEUROSCI.22-15-06309.2002 (2002).

27 Du, H. *et al.* Transcription Factors Bcl11a and Bcl11b Are Required for the Production and Differentiation of Cortical Projection Neurons. *Cerebral Cortex*, doi:10.1093/cercor/bhab437 (2021).

28 Li, Z. *et al.* BMP7 expression in mammalian cortical radial glial cells increases the length of the neurogenic period. *Protein Cell*, doi:10.1093/procel/pwad036 (2023).

29 Xu, Q., Tam, M. & Anderson, S. A. Fate mapping Nkx2.1-lineage cells in the mouse telencephalon. *J Comp Neurol* **506**, 16-29, doi:10.1002/cne.21529 (2008).

30 Floriddia, E. M. *et al.* Distinct oligodendrocyte populations have spatial preference and different responses to spinal cord injury. *Nat Commun* **11**, 5860, doi:10.1038/s41467-020-19453-x (2020).

31 Marques, S. *et al.* Oligodendrocyte heterogeneity in the mouse juvenile and adult central nervous system. *Science* **352**, 1326-1329, doi:10.1126/science.aaf6463 (2016).

32 Falcao, A. M. *et al.* Disease-specific oligodendrocyte lineage cells arise in multiple sclerosis. *Nat Med* **24**, 1837-1844, doi:10.1038/s41591-018-0236-y (2018).

33 Crawford, A. H., Tripathi, R. B., Richardson, W. D. & Franklin, R. J. M. Developmental Origin of Oligodendrocyte Lineage Cells Determines Response to Demyelination and Susceptibility to Age-Associated Functional Decline. *Cell Rep* **15**, 761-773, doi:10.1016/j.celrep.2016.03.069 (2016).

34 Yu, W.-P., Collarini, E. J., Pringle, N. P. & Richardson, W. D. Embryonic expression of myelin genes: Evidence for a focal source of oligodendrocyte precursors in the ventricular zone of the neural tube. *Neuron* **12**, 1353-1362, doi:https://doi.org/10.1016/0896-6273(94)90450-2 (1994).

513 35 Spassky, N. *et al.* Multiple restricted origin of oligodendrocytes. *J Neurosci* **18**, 8331-8343,
514 doi:10.1523/JNEUROSCI.18-20-08331.1998 (1998).
515 36 Fogarty, M., Richardson, W. D. & Kessaris, N. A subset of oligodendrocytes generated from
516 radial glia in the dorsal spinal cord. *Development* **132**, 1951-1959, doi:10.1242/dev.01777
517 (2005).
518 37 Orentas, D. M., Hayes, J. E., Dyer, K. L. & Miller, R. H. Sonic hedgehog signaling is required
519 during the appearance of spinal cord oligodendrocyte precursors. *Development* **126**,
520 2419-2429, doi:10.1242/dev.126.11.2419 %J Development (1999).
521 38 Lu, Q. R. *et al.* Sonic hedgehog--regulated oligodendrocyte lineage genes encoding bHLH
522 proteins in the mammalian central nervous system. *Neuron* **25**, 317-329,
523 doi:10.1016/s0896-6273(00)80897-1 (2000).
524 39 Flandin, P. *et al.* Lhx6 and Lhx8 coordinately induce neuronal expression of Shh that controls
525 the generation of interneuron progenitors. *Neuron* **70**, 939-950,
526 doi:10.1016/j.neuron.2011.04.020 (2011).
527 40 Tong, C. K. *et al.* A Dorsal SHH-Dependent Domain in the V-SVZ Produces Large Numbers of
528 Oligodendroglial Lineage Cells in the Postnatal Brain. *Stem Cell Reports* **5**, 461-470,
529 doi:10.1016/j.stemcr.2015.08.013 (2015).
530 41 Su, Z. *et al.* Dlx1/2-dependent expression of Meis2 promotes neuronal fate determination in
531 the mammalian striatum. *Development* **149**, doi:10.1242/dev.200035 (2022).
532 42 Dai, J., Bercury, K. K., Ahrendsen, J. T. & Macklin, W. B. Olig1 function is required for
533 oligodendrocyte differentiation in the mouse brain. *J Neurosci* **35**, 4386-4402,
534 doi:10.1523/JNEUROSCI.4962-14.2015 (2015).
535 43 Silbereis, J. C. *et al.* Olig1 function is required to repress dlx1/2 and interneuron production in
536 Mammalian brain. *Neuron* **81**, 574-587, doi:10.1016/j.neuron.2013.11.024 (2014).
537 44 Price, J. D. *et al.* DLX1 and the NuRD complex cooperate in enhancer decommissioning and
538 transcriptional repression. *Development* **149**, doi:10.1242/dev.199508 (2022).
539 45 Winkler, C. C. *et al.* The Dorsal Wave of Neocortical Oligodendrogenesis Begins Embryonically
540 and Requires Multiple Sources of Sonic Hedgehog. *J Neurosci* **38**, 5237-5250,
541 doi:10.1523/JNEUROSCI.3392-17.2018 (2018).
542 46 van Tilborg, E. *et al.* Origin and dynamics of oligodendrocytes in the developing brain:
543 Implications for perinatal white matter injury. *Glia* **66**, 221-238, doi:10.1002/glia.23256
544 (2018).
545 47 Windrem, M. S. *et al.* Human Glial Progenitor Cells Effectively Remyelinate the Demyelinated
546 Adult Brain. *Cell Rep* **31**, 107658, doi:10.1016/j.celrep.2020.107658 (2020).
547 48 Yang, L. *et al.* Transcriptional profiling reveals the transcription factor networks regulating the
548 survival of striatal neurons. *Cell death & disease* **12**, 262-262,
549 doi:10.1038/s41419-021-03552-8 (2021).

550

Figure legends:

Figure 1. Fate mapping of LGE-derived OPCs by combining IUE with a *Cre* recombinase-dependent *IS* reporter

(A) *In situ* hybridization showing *Pdgfra* expression from E13.5 to P0. Arrowheads indicated the *Pdgfra*$^+$ cell migration stream from the MGE/AEP to the cortex.

(B) Scheme of the *IS* reporter lines.

(C) Experimental schedule to trace LGE-derived OPCs.

(D) Representative coronal sections showing the distribution of tdT$^+$ cells.

(E) tdT$^+$ cells expressed NeuN but not OLIG2, SOX10, PDGFRA or NG2 in the cortex. In contrast, the tdT$^+$ cells expressed all of these markers (OLIG2, SOX10, PDGFRA, NG2 and NeuN) in the striatum.

(F) Fate mapping of LGE-derived cells at P0. tdT$^+$ cells expressed SOX10 and SOX9 in the striatum at P49.

Figure 2. Fate mapping of LGE-derived OPCs by combining IUE with PiggyBac transposon system

(A) Schematic of the PiggyBac transposon reporter system used in this study.

(B) The experimental workflow.

(C) Representative coronal sections showing the distribution of GFP$^+$ cells at E18.5.

(D) GFP^+ cells expressed NeuN but not glial cell markers, such as OLIG2, SOX10 and PDGFRA in the cortex. However, GFP^+ cells expressed NeuN, OLIG2, SOX10 and PDGFRA in the striatum.

(E) GFP^+ cells expressed NeuN but not glial cell markers, such as OLIG2, SOX10 and PDGFRA in the cortex and GFP^+ cells expressed NeuN, OLIG2, SOX10 and PDGFRA in the striatum at P10.

Figure 3. An exclusion strategy showed that cortical OPCs do not come from the LGE/CGE

(A) Scheme of the *H2B-GFP* reporter lines.

(B) Experimental design of the exclusion strategy to trace the lineage of LGE RGCs.

(C) Representative coronal sections showing the traced cells in the forebrain. The majority of SOX10- and PDGFRA-positive cells were GFP^+ cells in the cortex at P10.

(D-E) The pie chart shows that the percentage of LGE/dMGE-derived cortical OPCs was approximately 3%. N = 6 mice per group.

(F) Many GFP^+ cells expressed SOX10 and PDGFRA in the striatum at P10.

(G) Nearly all SOX10 and PDGFRA expressed GFP in the cortex at P0.

(H-I) The pie chart shows that the percentage of LGE/dMGE-derived cortical OPCs was less than 3%. N = 6 mice per group.

Figure 4. The MGE may be the sole ventral source of cortical OPCs

(A) The CRISPR/Cas9 technique was used to generate an *Olig2* conditional knockout allele.

(B) Experimental design for the generation of *Olig2-NCKO* mice.

(C-D) The expression of SOX10 and PDGFRA was significantly reduced in the cortex of *Olig2-NCKO* mice compared with that of control mice.

(E) The number of SOX10- and PDGFRA-positive cells was significantly reduced in *Olig2-NCKO* mice compared with control mice. Student's t-test, **P <.01, ***P <.001, n ≥ 5 mice per group, mean ± SEM.

(F) Few PDGFRA-positive cells were detected in the MGE/AEP of the *Olig2-NCKO* mice.

(G) A new model of the developmental origins of cortical OPCs.

Figure S1. Lineage tracing of LGE-derived OPCs by combining IUE with a *Cre* recombinase-dependent *IS* reporter

(A) Experimental schedule for fate mapping of LGE-derived OPCs.

(B) Representative coronal sections showing the distribution of the tdT^+ cells at P10.

(C) Nearly all tdT^+ cells expressed NeuN but not OLIG2 in the cortex. tdT^+ cells expressed NeuN and OLIG2 in the striatum.

(D) tdT^+ cells did not express OLIG2, SOX10, PDGFRA or ALDH1L1. Instead, they expressed NeuN in the cortex. In sharp contrast, tdT^+ cells in the striatum

expressed OLIG2, SOX10, PDGFRA, ALDH1L1 and NeuN at P10.

(E) 3D reconstruction of consecutive brain sections demonstrated that the traced cells were mainly located in the striatum.

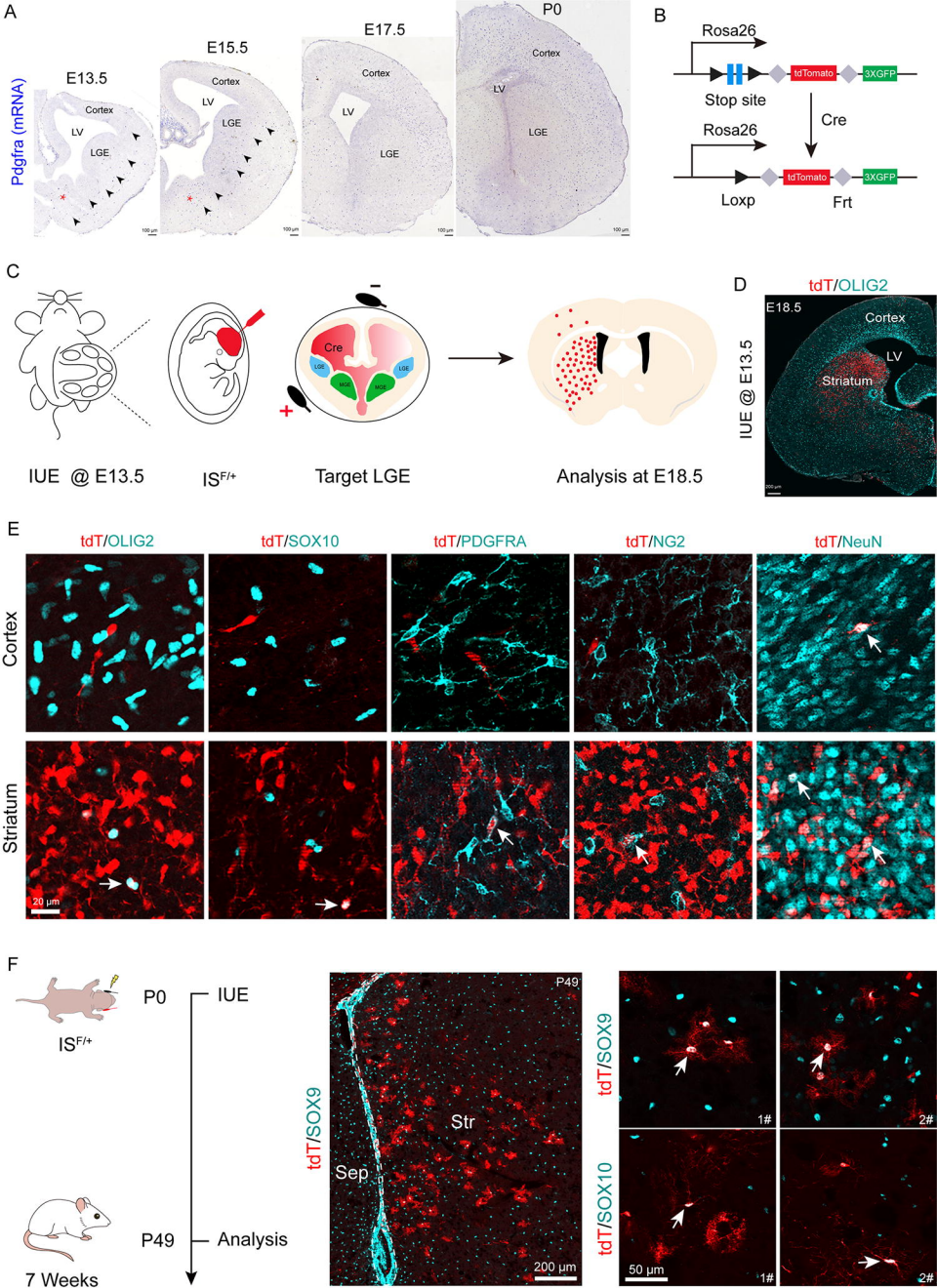
A
Pdgfra (mRNA)
E13.5
E15.5
E17.5
P0
Cortex
LV
LGE
B
Rosa26
Stop site
tdTomato
3XGFP
Cre
Loxp
Frt
C
IUE @ E13.5
IS^F/+
Target LGE
Analysis at E18.5
Cre
D
tdT/OLIG2
E18.5
Cortex
LV
Striatum
IUE @ E13.5
E
tdT/OLIG2
tdT/SOX10
tdT/PDGFRA
tdT/NG2
tdT/NeuN
Cortex
Striatum
20 μm
F
P0
IUE
IS^F/+
P49
Analysis
7 Weeks
tdT/SOX9
P49
Str
Sep
200 μm
tdT/SOX9
tdT/SOX10
1#
2#
50 μm

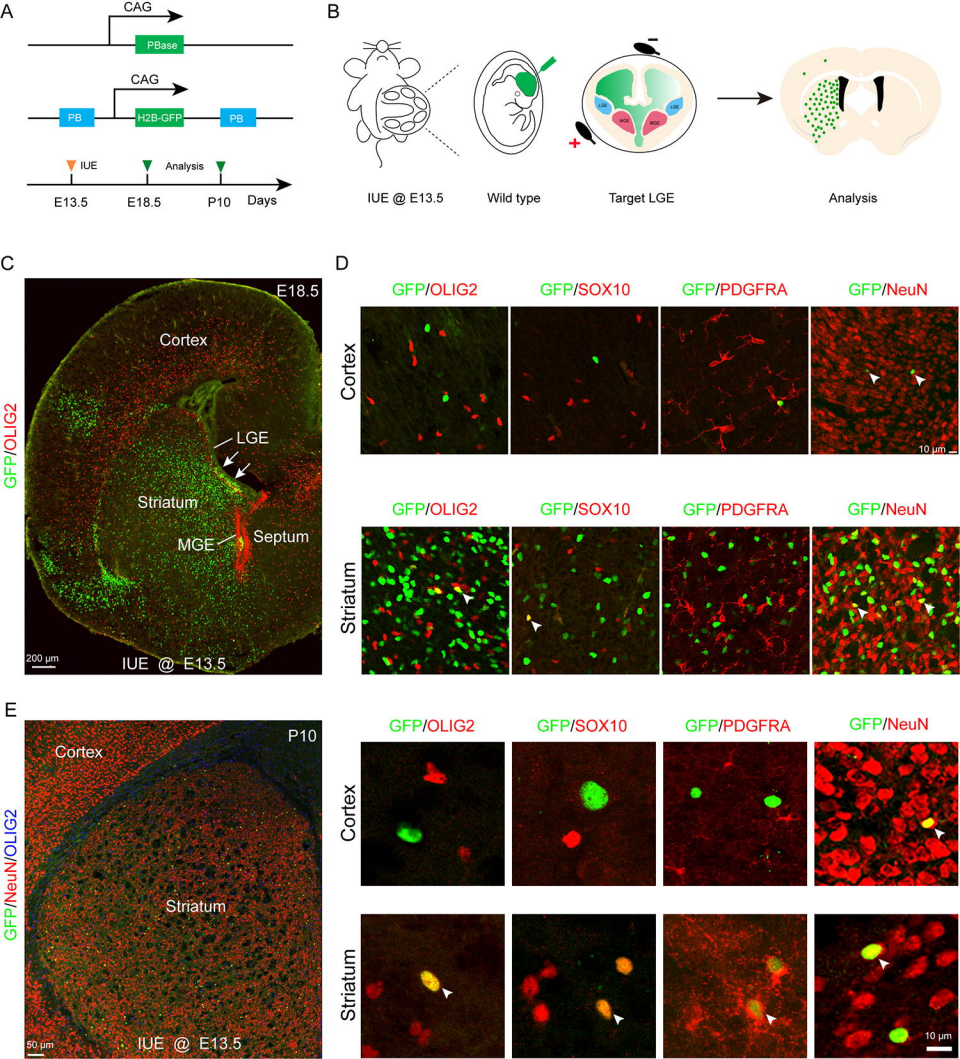
A
CAG
PBase
CAG
PB
H2B-GFP
PB
IUE
Analysis
E13.5
E18.5
P10
Days
B
IUE @ E13.5
Wild type
Target LGE
Analysis
C
E18.5
Cortex
LGE
Striatum
MGE
Septum
GFP/OLIG2
200 μm
IUE @ E13.5
D
GFP/OLIG2
GFP/SOX10
GFP/PDGFRA
GFP/NeuN
Cortex
Striatum
10 μm
E
P10
Cortex
Striatum
GFP/NeuN/OLIG2
50 μm
IUE @ E13.5
GFP/OLIG2
GFP/SOX10
GFP/PDGFRA
GFP/NeuN
Cortex
Striatum
10 μm

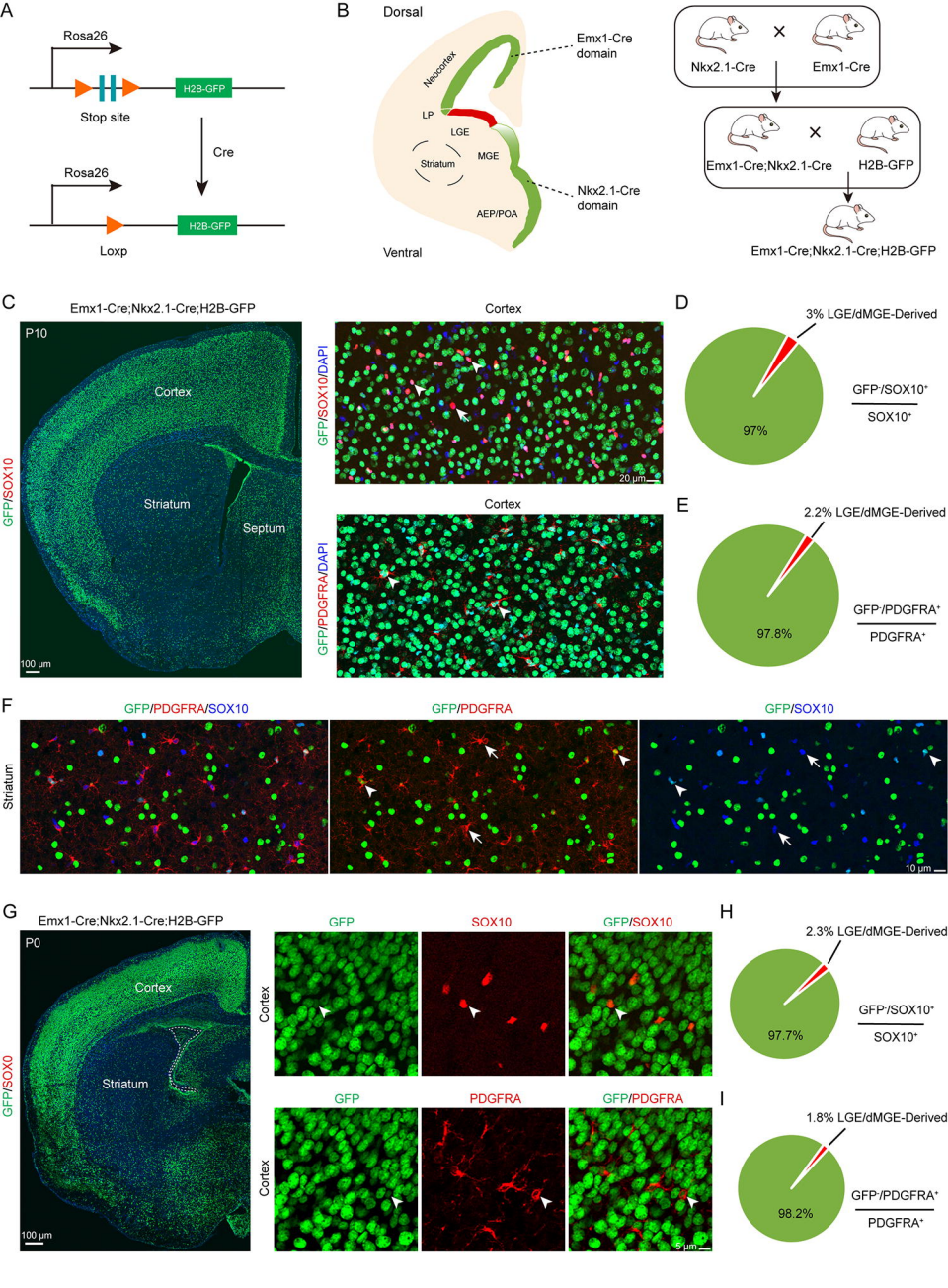
A
Rosa26
H2B-GFP
Stop site
Cre
Rosa26
H2B-GFP
Loxp
B
Dorsal
Neocortex
Emx1-Cre domain
LP
LGE
Striatum
MGE
Nkx2.1-Cre domain
AEP/POA
Ventral
Nkx2.1-Cre
Emx1-Cre
Emx1-Cre;Nkx2.1-Cre
H2B-GFP
Emx1-Cre;Nkx2.1-Cre;H2B-GFP
C
Emx1-Cre;Nkx2.1-Cre;H2B-GFP
P10
Cortex
Striatum
Septum
GFP/SOX10
100 μm
Cortex
GFP/SOX10/DAPI
20 μm
Cortex
GFP/PDGFRA/DAPI
D
3% LGE/dMGE-Derived
97%
GFP+/SOX10+
SOX10+
E
2.2% LGE/dMGE-Derived
97.8%
GFP+/PDGFRA+
PDGFRA+
F
GFP/PDGFRA/SOX10
GFP/PDGFRA
GFP/SOX10
Striatum
10 μm
G
Emx1-Cre;Nkx2.1-Cre;H2B-GFP
P0
Cortex
Striatum
GFP/SOX0
100 μm
GFP
SOX10
GFP/SOX10
Cortex
GFP
PDGFRA
GFP/PDGFRA
Cortex
H
2.3% LGE/dMGE-Derived
97.7%
GFP+/SOX10+
SOX10+
I
1.8% LGE/dMGE-Derived
98.2%
GFP+/PDGFRA+
PDGFRA+

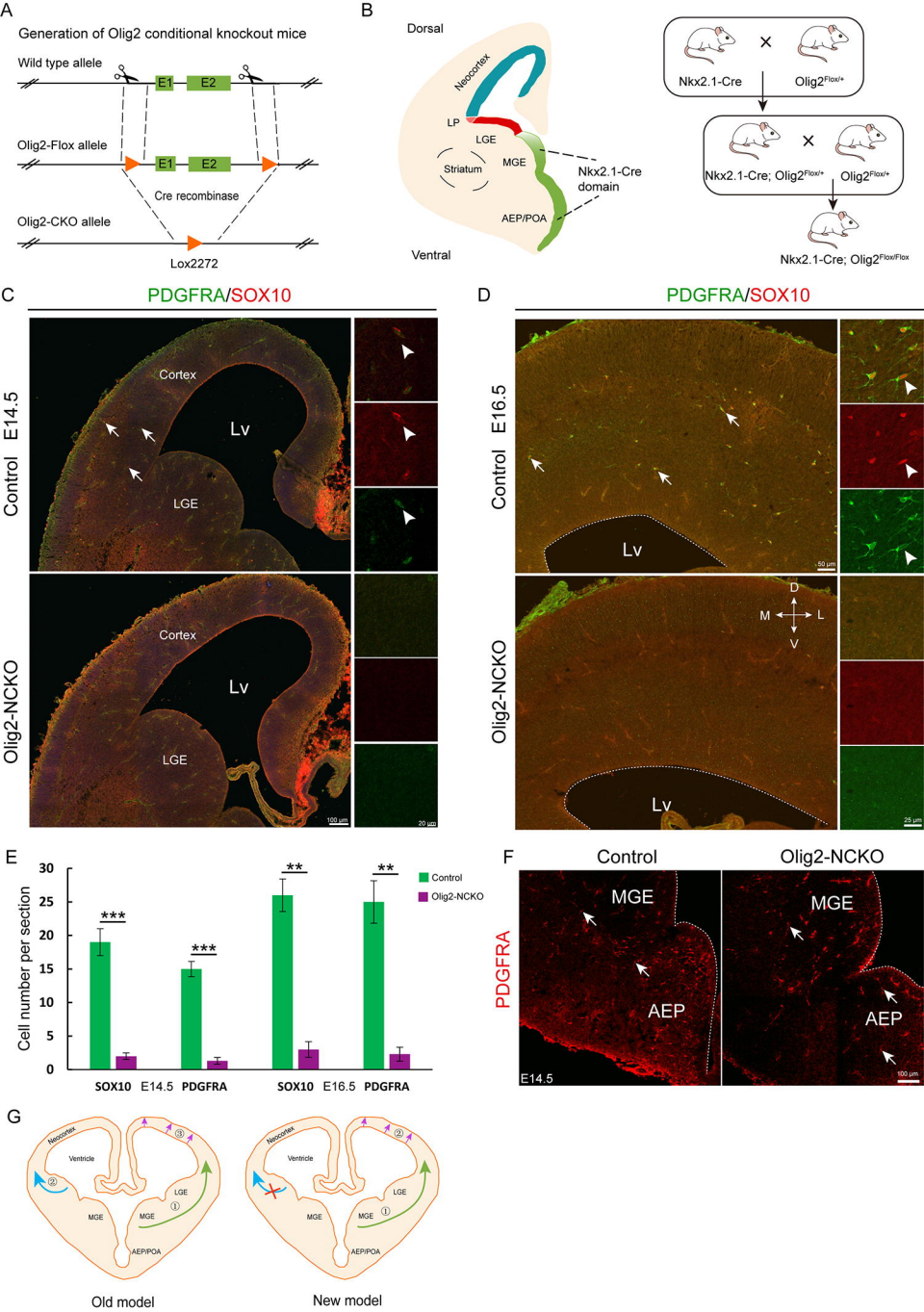
A
Generation of Olig2 conditional knockout mice
Wild type allele
E1
E2
Olig2-Flox allele
Cre recombinase
Olig2-CKO allele
Lox2272
B
Dorsal
Neocortex
LP
LGE
Striatum
MGE
AEP/POA
Nkx2.1-Cre domain
Ventral
Nkx2.1-Cre
Olig2Flox/+
Nkx2.1-Cre; Olig2Flox/+
Olig2Flox/+
Nkx2.1-Cre; Olig2Flox/Flox
C
PDGFRA/SOX10
Control E14.5
Olig2-NCKO
Cortex
Lv
LGE
100 μm
20 μm
D
PDGFRA/SOX10
Control E16.5
Olig2-NCKO
Lv
D
M
L
V
50 μm
25 μm
E
Cell number per section
Control
Olig2-NCKO
***
***
**
**
SOX10
E14.5
PDGFRA
SOX10
E16.5
PDGFRA
F
Control
Olig2-NCKO
PDGFRA
MGE
AEP
E14.5
100 μm
G
Neocortex
Ventricle
LGE
MGE
AEP/POA
Old model
New model